Direct observation of a pressure-induced metal-insulator transition in LiV_2O_4 by optical studies

A. Irizawa,* S. Suga,† and G. Isoyama
The Institute of Science and Industrial Research, Osaka University, Mihogaoka, Ibaraki, Osaka 567-0047, Japan

K. Shimai, K. Sato, K. Iizuka, and T. Nanba
Graduate School of Science and Technology, Kobe University, Higashinada, Hyogo 657-8501, Japan

A. Higashiya‡
RIKEN, Mikazuki, Sayo, Hyogo 679-5148, Japan

S. Niitaka
RIKEN, Hirosawa, Wako, Saitama 351-0198, Japan and
CREST, Japan Science and Technology Agency (JST), Kawaguchi, Saitama 332-0012, Japan

H. Takagi
RIKEN, Hirosawa, Wako, Saitama 351-0198, Japan,
CREST, Japan Science and Technology Agency (JST), Kawaguchi, Saitama 332-0012, Japan, and
Department of Advanced Materials Science, The University of Tokyo, Kashiwanoha, Kashiwa, Chiba 277-8581, Japan

(Received 4 July 2011; revised manuscript received 7 November 2011; published 5 December 2011)

The metal-insulator (MI) transition in LiV_2O_4 has been studied by optical measurements in infrared regions at low temperatures and under high pressures. At 40 K, the metal phase under ambient pressure changes gradually into the insulating state under pressures above 7 GPa, where the newly opened 2Δ gap is estimated to be $\sim$0.4 eV. At pressures higher than 8 GPa, the precursor of the structural phase transition is observed as a redshift of the transverse optical phonon peak in the far-infrared (FIR) region with decreasing temperatures. The behavior of this pressure-induced MI transition is observed not only at low temperatures but also at room temperature. At 300 K, a decrease in conduction carriers with pressure is also detected as a gradual suppression in the Drude response of the FIR region below 0.1 eV, with a ten- to 20-fold decrease in the optical conductivity. Extensive investigation of the optical response revealed a successive transformation of the electronic state in a region between the metal and the insulator phases in the pressure-temperature phase diagram. The redshift is only observed near the boundary to the insulator phase (boundary 2), where a complete homogeneous structural change appears to occur. On the contrary, an inhomogeneous structural change is realized in the intermediate phase between the metal and insulator phases, between boundaries 1 and 2, accompanied by a topographic localization or a short-range alternation of the valence.

DOI: 10.1103/PhysRevB.84.235116 PACS number(s): 71.27.+a, 71.30.+h, 78.30.−j, 81.40.Tv

I. INTRODUCTION

The heavy fermion (HF) state in $3d$ electron transition-metal oxides is one of the most attractive topics in solid-state physics from the viewpoint of unique Kondo mechanisms. The general Kondo mechanism of f-electron systems requires both the conduction electron and localized f electron, in which c-f hybridization between the conduction and f electrons is responsible for the spin-singlet state. On the contrary, another scenario can be proposed to explain the Kondo mechanism in d-electron systems because of the itinerancy of d electrons. Scenarios such as the frustrated spin interaction, nearly magnetic state with a strongly degenerated ground state, and deformation of the valence band with both itinerant and localized characters have so far been considered.

These scenarios have been examined over the past decade by theories and experiments to explain the low-temperature Fermi-liquid behavior in the ternary transition-metal oxide LiV_2O_4.[1–28] The first HF behavior in a $3d$-electron system was found in this compound.[29,30] This compound has a spinel structure, with the nearest-neighbor vanadium triangular network forming the pyrochlore-type sublattice. Among considerable spinel systems, only a few have been found to exhibit metallic behavior. In the early studies of the polycrystalline samples, the precise solid-state properties of LiV_2O_4 were unclear.[1,2,6,7,29–33] Clear evidence of metallicity and HF behavior have been obtained with single crystals.[34–39] With regard to the Kadowaki-Woods relation, large values of $A = 2.0\ \mu\Omega\ \mathrm{cm/K^2}$ for the coefficient of the T^2 term in the electrical resistivity $\rho(T)$ and $\gamma \sim 350\ \mathrm{mJ/mol\ K^2}$ for the coefficient of the electronic specific heat are comparable to those of the typical HF compound UPt_3.[36] Optical reflectivity under ambient pressure shows a noticeable change in the Drude response in a wide energy range up to 1 eV with a decrease in temperature to 6 K.[40] Although the magnetic susceptibility showed Curie-Weiss-like behavior due to a localized magnetic moment, there was no sign of long-range magnetic ordering down to 20 mK, in spite of a short-range magnetic correlation below 20 K. Hence, from a macroscopic perspective, the low-temperature ground state of LiV_2O_4 appears to be similar to that of the common f-electron HF systems under ambient pressure.

However, under high pressures and low temperatures, the characteristic electronic properties of LiV_2O_4 change drastically from those of a typical HF metal to those of a peculiar insulator.[41,42] The metallic behavior in the electrical resistivity changes into the insulating behavior above 6 GPa, at which the resistivities exhibit complex curvatures with several steps as a function of temperature. In the ρ-T curve at 8.5 GPa, the gradient $d\rho/dT$ changes continuously from a positive value to a negative value below 220 K and changes to a slower negative value below 70 K.[41] X-ray diffraction (XRD) experiments on the powder sample have revealed that the crystal symmetry changes from a cubic to a rhombohedral structure with decreasing temperature during the pressure-induced MI transition.[43] A similar structural distortion has been found in the associated spinel compound AlV_2O_4 that is in an insulating state at room temperature and under ambient pressure.[44,45] In AlV_2O_4, the valence number alternates spatially as $V^{2+}(d^3) : V^{3+}(d^2) = 1 : 1$, and the so-called charge-ordering (CO) state is realized. Hence, one can conceive that under high pressures LiV_2O_4 is likely to be in the CO state, in which the valence number might alternate as $V^{3+}(d^2) : V^{4+}(d^1) = 1 : 1$ or $V^{3+}(d^2) : V^{5+}(d^0) = 3 : 1$. Indeed, under pressures greater than 13 GPa at room temperature, an extended x-ray absorption fine structure (EXAFS) experiment revealed that the distribution of the V-V bond length could be explained by considering the formation of a cluster of seven vanadium atoms, as proposed for the CO state in AlV_2O_4.[46,47] ^{7}Li NMR studies at low temperatures and under pressures up to 4.74 GPa have further demonstrated the enhancement of an antiferromagnetic spin correlation in LiV_2O_4.[48,49]

The purpose of this paper is to examine the change in the electronic state of LiV_2O_4 from the normal HF state under ambient pressure to the insulating state under high pressures. We have measured the optical reflectivity of LiV_2O_4 under high pressures and at low temperatures by using infrared microscopes tuned to multiextreme conditions. The optical conductivity spectra derived from the reflectivity spectra were analyzed, and the MI transition involving the lattice deformation is demonstrated.

II. EXPERIMENTAL DETAILS

All the optical experiments were performed on the fractured mirror surfaces of LiV_2O_4 single crystals. The reflectivity measurements under multiextreme conditions were carried out on the infrared microscopes. The far-infrared (FIR) region was covered by the synchrotron radiation at the beamline BL43IR in SPring-8 (0.025–0.1 eV).[50,51] The higher-energy regions, i.e., midinfrared (MIR), near-infrared (NIR), and visible (VIS) regions (0.1–2.5 eV) were covered by conventional light sources in the university laboratory.[52] The temperature between 10 and 300 K was covered by a liquid-He flow-type refrigeration unit built into a cryostat. High pressures up to 20 GPa were applied by a diamond-anvil cell (DAC), in which the sample and the ruby fragments for pressure calibration were set on the flat diamond surface (culet) with a 0.6 mm ϕ diameter, together with Au foil that was used as a standard reflector in the same optical alignment. They were enclosed within the pressure medium by a stainless-steel gasket. To avoid the pressure-distribution effect, we paid attention to the measuring conditions. At first all the pressuring processes were executed at room temperature, and then the sample temperature was changed. The samples were placed at the center of the culet of the DAC with the pressure medium Daphne 7373.[53,54] Then the reproducibility of the spectra was carefully verified. The standard spectrum, namely, the reflectivity under ambient pressure, was measured by a Fourier-transform-type spectrometer IFS-66v (Bruker Optics). The optical conductivity spectra were derived from the reflectivity spectra with the standard Kramers-Kronig (KK) transformation.

III. RESULTS AND DISCUSSION

Figures 1(a) and 1(b) summarize the dependence of the reflectivity and optical conductivity on pressures at 40 K. The reflectivity and the optical conductivity (σ) are shown for a typical case of the pressure-induced MI transition. Under ambient pressure, the optical spectrum represents a metallic state with a finite Drude response, which is consistent with the results of previous reports on the electrical resistivity and the optical response of LiV_2O_4.[36,40] On applying a high pressure, the spectrum changes drastically from the initial spectrum observed under ambient pressure. The reflectivity starts to change from ~5 GPa, together with a decreasing Drude response over a wide energy range extending from ~0.1 to 1.5 eV [see Fig. 1(a)]. In the optical conductivity spectra in Fig. 1(b), a hump appears gradually in the MIR region (0.3–1.5 eV) under pressures above 8 GPa. A clear hump is

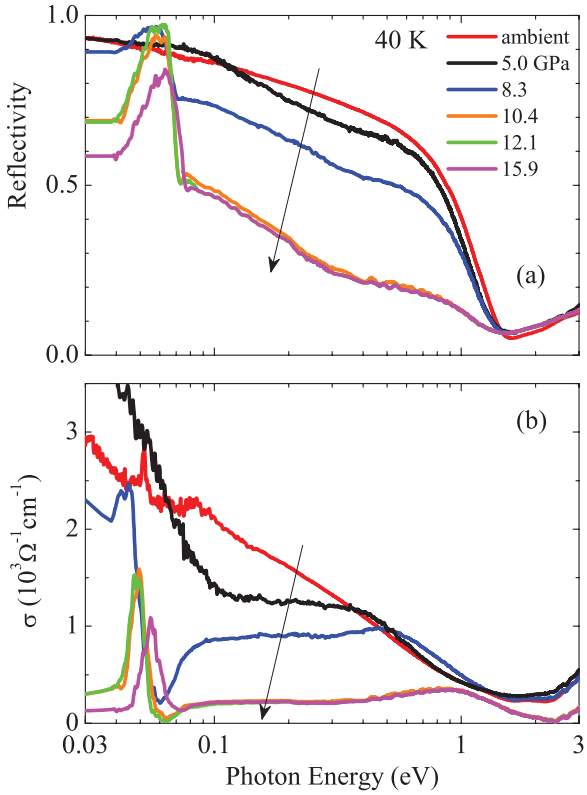

FIG. 1. (Color online) Pressure dependence on the reflectivity (a) and the optical conductivity (b) of LiV_2O_4 at 40 K.

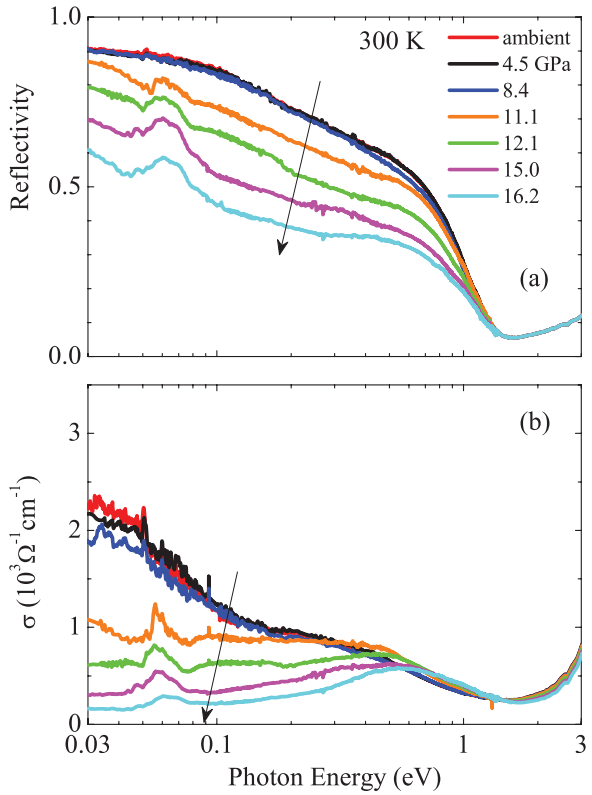

FIG. 2. (Color online) Pressure dependence on the reflectivity (a) and the optical conductivity (b) of LiV_2O_4 at 300 K.

observed at ∼1 eV under pressures above 10 GPa. This hump is interpreted as an interband transition. A 2Δ band gap is estimated to be ∼0.4 eV from the low-energy rising edge of this hump.

Although the electrical resistivity shows only a small pressure dependence, an interesting pressure effect was found in this study, even at 300 K. In Figs. 2(a) and 2(b), the spectra show gradual but clear changes toward an insulating state under high pressures. The Drude response starts to change under pressures above 9 GPa, and the change continues up to the present experimental limit of 20 GPa. Similar to the σ spectra at 40 K, a hump grows in the σ spectra at 300 K under pressures above 9 GPa in the region between 0.5 and 0.6 eV. This means that a MI change takes place in this compound under high pressures not only at low temperatures but also at room temperature. The difference from the low-temperature results is that the MI change at 300 K is continuous up to 17 GPa, whereas at low temperatures both reflectivity and σ spectra do not change much at pressures above 10 GPa in the region above 0.1 eV. This gradual change at 300 K is related to the spectral change at 40 K between ∼5 and 10 GPa, as shown in Fig. 3. Focusing on the results in the FIR region, there is a prominent peak associated with the IR-active F_{1u} phonon in a cubic spinel at ∼0.05 eV.[40,55] This phonon becomes broader with a decrease in the Drude component under higher pressures at both 40 and 300 K, as demonstrated by the σ spectra in Figs. 1(b) and 2(b). Such a broadened phonon structure is typically observed in ionic insulators such as alkali halides and is known as a residual ray band and/or reststrahlen band.

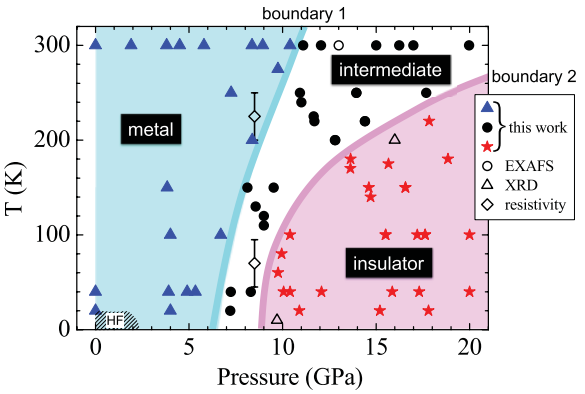

FIG. 3. (Color online) Pressure-temperature phase diagram of LiV_2O_4. Three regions (metal—filled triangles; intermediate—filled circles; and insulator—filled stars) with two boundaries (boundary 1 and 2) are determined by the optical response. The HF state is located in the bottom left-hand-side area (shaded) and is estimated from the NMR experiment (Refs. 48 and 49). The characteristic points from the other experiments are also plotted in the figure [EXAFS (Ref. 47)—open circles; XRD (Ref. 43)—open triangles; and resistivity (Ref. 41)—open diamonds).

Summarizing the results of our experiments, the electronic states can be classified in the pressure-temperature (P-T) phase diagram in Fig. 3. There are three distinct regions and two boundaries based on the observed electronic properties. In addition to the metal phase under low pressures and the insulator phase under high pressures, there is certainly an intermediate phase that exists between the metal phase and the insulator phase. Our experimental results are shown by filled triangles, filled circles, and filled star symbols. There are two boundaries: one between the metal and the intermediate regions (boundary 1), and the other between the intermediate and the insulator regions (boundary 2). These regions are determined from the behavior of the optical spectra as follows. In the metal phase, the Drude responses in the reflectivity spectra maintain the spectral shape with temperature and pressure. In the insulating phase at low temperatures, spectra above 0.1 eV show a very poor response to pressure. In the intermediate phase, the spectra show a gradual change from those of the metal to those of the insulator with pressure. We also plot the critical points found in previous studies of the electrical and structural changes in LiV_2O_4 with open symbols. These critical points correspond to the structural phase transition observed in the EXAFS experiment (open circles),[46,47] the (440) diffraction peak splitting in the XRD experiment (open triangles),[43] and the minimum and kink in the electrical resistivity at 8.5 GPa (open diamonds).[41,42] According to this phase diagram, the structural changes observed in the EXAFS and the XRD experiments correlate well with boundaries 1 and 2. The minimum and the kink points observed in the electrical resistivity are also located near boundaries 1 and 2, respectively. It can be concluded from these results that the progress in the localization of conduction electrons is closely related to the structural changes that take place near the two boundaries. Subsequently, we investigate the pressure-induced structural phase transitions based on the details of the phonon-softening behavior in the optical spectra.

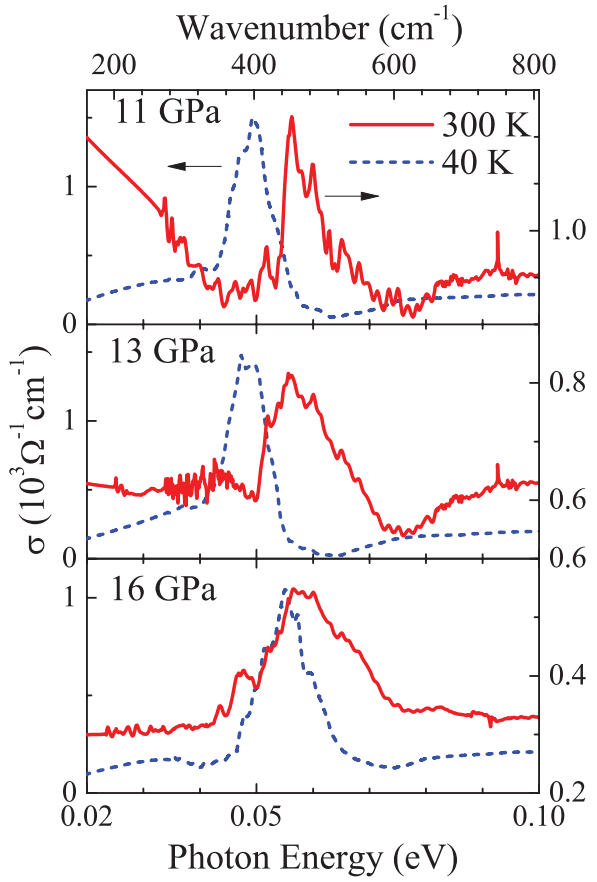

FIG. 4. (Color online) Phonon softening phenomenon observed in the optical spectra at 11, 13, and 16 GPa.

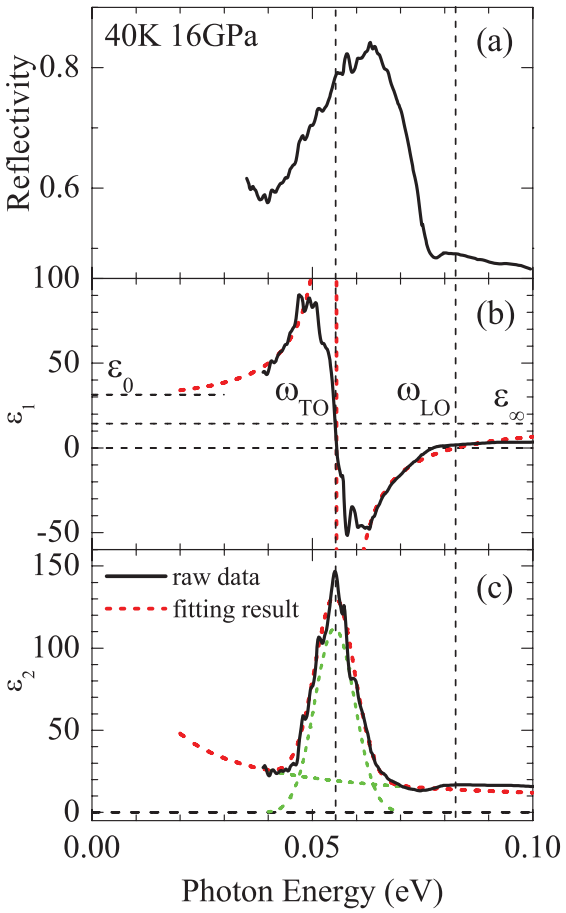

FIG. 5. (Color online) Kramers-Kronig analysis of the reflectivity spectrum (a) to derive the imaginary and real parts of the dielectric function ϵ_1, ϵ_2 [(b), (c), respectively] at 40 K and 16 GPa. The estimated ω_{TO}, ω_{LO}, ϵ_0, and ϵ_∞ from fitting results (dashed lines) are also indicated with experimental results (solid lines) in figures.

A decrease in temperature generally results in crystal-lattice shrinkage, which causes hardening of the crystal and shifting of phonon peaks toward higher energies in optical spectra. Figure 4 represents the typical phonon behavior with temperature at high pressures. It must be noted that the peak position under each pressure shifts clearly toward lower energies, when the temperature decreases from 300 to 40 K. This phonon behavior is well known as a phonon-softening phenomenon, which is a freezing process of the specific phonon mode toward the structural phase transition.

The transverse optical phonon frequency ω_{TO} can be estimated from the dielectric function in each pressure-induced insulating phase. For instance, Fig. 5 represents the reflectivity (a) and the real and imaginary parts of the dielectric function [(b) ϵ_1 and (c) ϵ_2] at 40 K and 16 GPa. The static $\epsilon(0)$ and $\epsilon(\infty)$ can be further obtained from the extrapolations of ϵ_1. The longitudinal optical phonon frequency ω_{LO} and the transverse optical phonon frequency ω_{TO} can be estimated from the wave numbers at the zero-cross points of ϵ_1 and at the peak position in ϵ_2, respectively, as shown in Figs. 5(b) and 5(c). All the curves of ϵ_2 around ω_{TO} are well fitted by a single Gaussian peak and a background as shown in Fig. 5(c). The obtained parameters comply well with the Lyddane-Sachs-Teller (LST) relation, described as $\omega_{TO}^2/\omega_{LO}^2 = \epsilon(\infty)/\epsilon(0)$. The relation denotes that this pressure-induced insulating phase is in a unitary and ideal ionic state.

In this manner, the temperature dependence of ω_{TO} as a function of pressure is shown in Fig. 6. In the metallic phase under ambient pressure, the phonon peak frequency ω_{TO} shifts monotonously toward higher energies with decreasing temperature, due to the phonon-hardening phenomenon. Although the phonon-hardening phenomenon is also observed for 13 and 16 GPa at high temperatures, the steep drop in ω_{TO} occurs below ~200 K due to a phonon-softening phenomenon. At pressure of 8 GPa, the ω_{TO} increases in the metallic phase with decreasing temperature and stays almost constant in the intermediate phase. The results in Fig. 6 demonstrate the completion of the structural phase transition under high pressures accompanied by phonon softening, which takes place near boundary 2. One of the likely scenarios for the change in the intermediate phase is the development of insulator grains in the metal. Short-range charge localization develops in the insulator grains in the intermediate phase and fully occupies the whole crystal in the insulator phase. Under high pressures and sufficiently low temperatures, the insulator phase is stabilized without noticeable spectral changes. Other experimental results obtained from previous studies also support this scenario, and can be explained as follows. For

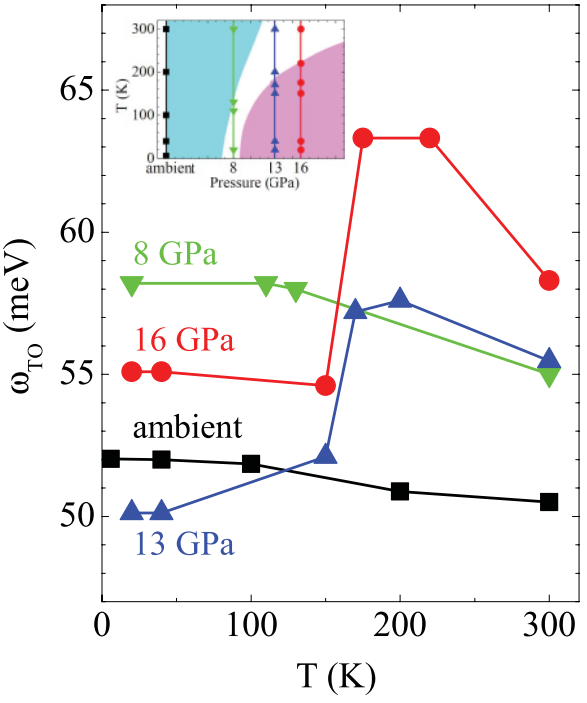

FIG. 6. (Color online) Changes of ω_{TO} as a function of the temperature under 0 (ambient pressure), 8, 13, and 16 GPa.

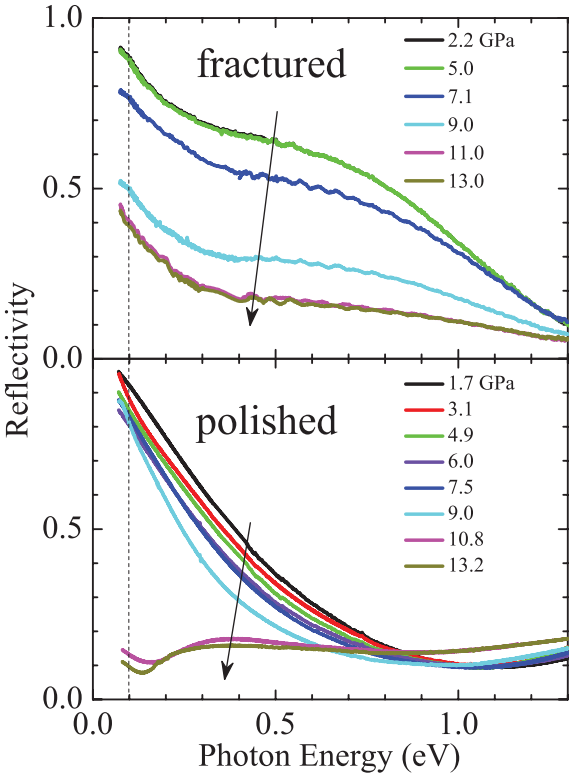

FIG. 7. (Color online) Pressure dependence on the reflectivity of the fractured (a) and the polished (b) surfaces in MIR region at 40 K. The dashed line drawn at 0.1 eV is a guide for the intensity plot in Fig. 8.

electrical resistivity, two characteristic transformations are recognized at 8.5 GPa, as indicated by the open diamonds in Fig. 3.[41,42] One is the metal-insulator change at ~220 K, in which the slope changes gradually from positive to negative with decreasing temperature, and the second is the insulator-insulator change at ~70 K, in which the gradient of the negative slope decreases at lower temperatures. These transformations can be understood by considering the changes in electronic states; the former is ascribed to the starting point of the charge localization (220 K) and the latter is ascribed to the decay in the electron scattering induced by the randomness in the intermediate phase during the transition to the insulator phase (70 K). From a structural perspective, the short-range charge localization in the intermediate phase may be accompanied by a spatial fluctuation of the bond length, resulting in a partial distortion of the crystal. At room temperature, the structural distortion observed in the EXAFS experiment starts at a pressure of 12 GPa near boundary 1.[46,47] The microscopic rearrangement of the atoms results in minimal insulator grains at 12 GPa, and an increase in the size and/or number of grains takes place in the intermediate phase at pressures above 12 GPa. Moreover, the structural transition observed in the XRD measurement (at 10 K and 9.7 GPa, and at 200 K and 16 GPa) also indicates the completion of the growth of this partial distortion through the crystal near boundary 2.[43]

Finally, we show the details of the surface sensitivity of this compound that were reported in previous studies.[40,56,57] Figure 7 demonstrates a clear difference in the pressure dependence of the MIR reflectivity of both fractured and polished surfaces. These changes are reproducible for all polishing treatments on the surfaces of different crystals. These changes are not due to a simple phenomenon such as a surface contamination, which is often found in surface-sensitive experiments.[58–60] A metallic state obviously exists *in* the polished sample at low pressures. Although the reflectivity decreases up to 1 eV on both surfaces, the plasma edge is transformed and shifted to lower energies on the polished surface. The dependence of reflectivity on pressures is much larger for the fractured surfaces in the 0.3–0.9 eV region. The intensity of the reflectivity at 0.1 eV is plotted as a function of the pressure in Fig. 8. Some significant differences are recognized between the fractured and polished surfaces. The change in the reflectivity from ambient pressure to high pressures is much smaller for the fractured surface. The transition pressure is higher and the change is steeper for the polished surface. These results demonstrate that the polishing treatment changes the electronic state at least down to several micrometers from the surface, which is comparable to the wavelength of infrared light. One possible reason for such deterioration is that the minimum of total energy under ambient pressure, including lattice vibration, charge, and magnetic interactions and so on, of this compound is located near the critical point of the structural phase transition. Then the transition may be triggered by the polishing treatment due to ionic defects and/or lattice imperfections.[61] Therefore, attention must be paid to experimental sample preparation involving powdering and even trimming of surfaces.

Although the electronic state under ambient pressure is not much discussed in this paper, the HF state in LiV_2O_4 originates most probably from the eccentric electron ground state, which is intrinsically involved in a charge fluctuation and

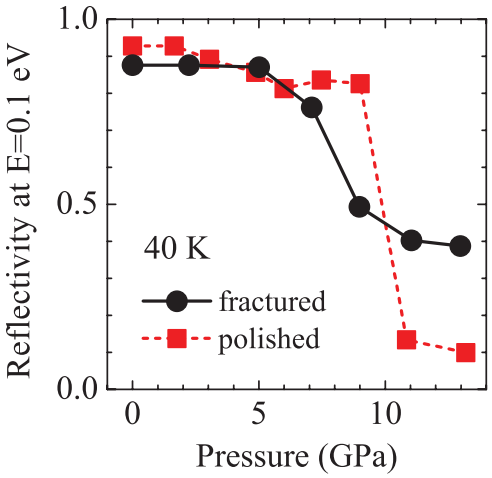

FIG. 8. (Color online) Pressure dependence on the intensity of the reflectivity at $E = 0.1$ eV on the fractured and the polished surfaces. See also the caption of Fig. 7.

an antiferromagnetic spin fluctuation as a result of the strong electron correlation. This HF state is located next to the two non-Fermi-liquid states at low temperatures. On the one hand, the insulator state is stabilized above 9 GPa at low temperature, as confirmed by our experiments, and never shows a metallic state with increasing pressure (to a maximum of 20 GPa). Considering the similarity between the crystal structures, the charge fluctuation nature of AlV_2O_4 resulting in charge ordering below 700 K (Ref. 44) is expected to occur in the pressure-induced insulator phase of LiV_2O_4. Photoemission spectroscopy experiments also suggest the importance of the hybridization between the O $2p$ states and the V $3d$ states in forming the HF state.[57,62] On the other hand, the NMR nuclear relaxation rate T_1 in LiV_2O_4 above 2.3 GPa ($\leqslant$4.74 GPa) and below 20 K ($\geqslant$60 mK) shows a deviation from the Korringa relation of $T_1T = \text{const.}$, which is characteristic of the normal Fermi-liquid state.[48,49] Although no magnetic ordering is observed in this pressure-temperature region, the increment of $1/T_1T$ as a function of pressure denotes the development of the antiferromagnetic spin interaction between the V ions. Consequently, the stability of these two non-Fermi-liquid natures, namely, charge fluctuation and spin fluctuation under high pressures strongly implies the unique origin of the HF state in this $3d$-based compound. According to the dynamic change in electrical conduction[41,42] compared to the rather moderate change in the magnetization as a function of pressure,[48,49] the delicate balance of the charge distribution, together with the triangular antiferromagnetic spin frustration, may be the key to understanding the nature of HF state under ambient pressure of this compound.

IV. SUMMARY

Optical studies in the infrared region were carried out on the $3d$-electron oxide LiV_2O_4 under high pressures and low temperatures. High pressures up to 20 GPa induced a stable ionic insulator phase at low temperatures. An intermediate phase containing features of both metallic conduction and ionic charge localization exists between the metal phase under low pressures and the ionic insulator phase under high pressures. The phonon-softening phenomenon, as a precursor of the macroscopic structural phase transition, can be ascertained only near the boundary between the intermediate and the insulator phases.

ACKNOWLEDGMENTS

The authors would like to thank T. Moriwaki and Y. Ikemoto, the staff of SPring-8/JASRI, for their technical support. We also acknowledge M. Matsunami for valuable discussions. This work was partly supported by KAKENHI (13354003, 19560665, 19654043, and 22560659).

*irizawa@sanken.osaka-u.ac.jp
†Graduate School of Engineering Science, Osaka University, Machikaneyama, Toyonaka, Osaka 560-8531, Japan.
‡Industrial Technology Center of Wakayama Prefecture, Kokura, Wakayama, Wakayama 649-6261, Japan.

[1] A. V. Mahajan, R. Sala, E. Lee, F. Borsa, S. Kondo, and D. C. Johnston, Phys. Rev. B **57**, 8890 (1998).
[2] A. Krimmel, A. Loidl, M. Klemm, S. Horn, and H. Schober, Phys. Rev. Lett. **82**, 2919 (1999).
[3] V. Eyert, K. H. Höck, S. Horn, A. Loidl, and P. S. Riseborough, Europhys. Lett. **46**, 762 (1999).
[4] V. I. Anisimov, M. A. Korotin, M. Zölfl, T. Pruschke, K. Le Hur, and T. M. Rice, Phys. Rev. Lett. **83**, 364 (1999).
[5] J. Matsuno, A. Fujimori, and L. F. Mattheiss, Phys. Rev. B **60**, 1607 (1999).
[6] D. C. Johnston, C. A. Swenson, and S. Kondo, Phys. Rev. B **59**, 2627 (1999).
[7] S. Kondo, D. C. Johnston, and L. L. Miller, Phys. Rev. B **59**, 2609 (1999).
[8] C. M. Varma, Phys. Rev. B **60**, R6973 (1999).
[9] D. J. Singh, P. Blaha, K. Schwarz, and I. I. Mazin, Phys. Rev. B **60**, 16359 (1999).
[10] H. Kusunose, S. Yotsuhashi, and K. Miyake, Phys. Rev. B **62**, 4403 (2000).
[11] A. P. Murani, Phys. Rev. Lett. **85**, 3981 (2000).
[12] S. H. Lee, Y. Qiu, C. Broholm, Y. Ueda, and J. J. Rush, Phys. Rev. Lett. **86**, 5554 (2001).
[13] S. Fujimoto, Phys. Rev. B **65**, 155108 (2002).
[14] S. Burdin, D. R. Grempel, and A. Georges, Phys. Rev. B **66**, 045111 (2002).
[15] J. Hopkinson and P. Coleman, Phys. Rev. Lett. **89**, 267201 (2002).
[16] Y. Yamashita and K. Ueda, Phys. Rev. B **67**, 195107 (2003).
[17] I. A. Nekrasov, Z. V. Pchelkina, G. Keller, T. Pruschke, K. Held, A. Krimmel, D. Vollhardt, and V. I. Anisimov, Phys. Rev. B **67**, 085111 (2003).
[18] M. S. Laad, L. Craco, and E. Müller-Hartmann, Phys. Rev. B **67**, 033105 (2003).
[19] J. D. Lee, Phys. Rev. B **67**, 153108 (2003).
[20] N. Tsujii, K. Yoshimura, K. Kosuge, H. Mitamura, and T. Goto, J. Phys. Condens. Matter **15**, 185 (2003).

[21] A. Koda, R. Kadono, W. Higemoto, K. Ohishi, H. Ueda, C. Urano, S. Kondo, M. Nohara, and H. Takagi, Phys. Rev. B **69**, 012402 (2004).
[22] V. Yushankhai, P. Fulde, and P. Thalmeier, Phys. Rev. B **71**, 245108 (2005).
[23] K. Takubo, J.-Y. Son, T. Mizokawa, H. Ueda, M. Isobe, Y. Matsushita, and Y. Ueda, Phys. Rev. B **74**, 155103 (2006).
[24] R. Arita, K. Held, A. V. Lukoyanov, and V. I. Anisimov, Phys. Rev. Lett. **98**, 166402 (2007).
[25] V. Yushankhai, A. Yaresko, P. Fulde, and P. Thalmeier, Phys. Rev. B **76**, 085111 (2007).
[26] V. Yushankhai, P. Thalmeier, and T. Takimoto, Phys. Rev. B **77**, 125126 (2008).
[27] K. Hattori and H. Tsunetsugu, Phys. Rev. B **79**, 035115 (2009).
[28] V. Yushankhai, T. Takimoto, and P. Thalmeier, Phys. Rev. B **82**, 085112 (2010).
[29] S. Kondo, D. C. Johnston, C. A. Swenson, F. Borsa, A. V. Mahajan, L. L. Miller, T. Gu, A. I. Goldman, M. B. Maple, D. A. Gajewski, E. J. Freeman, N. R. Dilley, R. P. Dickey, J. Merrin, K. Kojima, G. M. Luke, Y. J. Uemura, O. Chmaissem, and J. D. Jorgensen, Phys. Rev. Lett. **78**, 3729 (1997).
[30] O. Chmaissem, J. D. Jorgensen, S. Kondo, and D. C. Johnston, Phys. Rev. Lett. **79**, 4866 (1997).
[31] O. Faran and V. Volterra, Solid State Commun. **101**, 861 (1997).
[32] M. Onoda, H. Imai, Y. Amako, and H. Nagasawa, Phys. Rev. B **56**, 3760 (1997).
[33] N. Fujiwara, H. Yasuoka, and Y. Ueda, Phys. Rev. B **57**, 3539 (1998).
[34] D. B. Rogers, J. L. Gillson, and T. E. Gier, Solid State Commun. **5**, 263 (1967).
[35] H. Takagi, C. Urano, S. Kondo, M. Nohara, Y. Ueda, T. Shiraki, and T. Okubo, Mater. Sci. Eng. B **63**, 147 (1999).
[36] C. Urano, M. Nohara, S. Kondo, F. Sakai, H. Takagi, T. Shiraki, and T. Okubo, Phys. Rev. Lett. **85**, 1052 (2000).
[37] Y. Matsushita, H. Ueda, and Y. Ueda, Nat. Mater. **4**, 845 (2005).
[38] A. Shimoyamada, S. Tsuda, K. Ishizaka, T. Kiss, T. Shimojima, T. Togashi, S. Watanabe, C. Q. Zhang, C. T. Chen, Y. Matsushita, H. Ueda, Y. Ueda, and S. Shin, Phys. Rev. Lett. **96**, 026403 (2006).
[39] S. Das, X. Zong, A. Niazi, A. Ellern, J. Q. Yan, and D. C. Johnston, Phys. Rev. B **76**, 054418 (2007).
[40] P. E. Jönsson, K. Takenaka, S. Niitaka, T. Sasagawa, S. Sugai, and H. Takagi, Phys. Rev. Lett. **99**, 167402 (2007).
[41] C. Urano, Ph.D. thesis, The University of Tokyo, 2000.
[42] S. Niitaka, N. Dragoe, L. Pinsard-Gaudart, J. Itie, A. Congeduti, P. Roy, P. Lagarde, A. Flank, and H. Takagi, "EXAFS study of LiV_2O_4 under high pressure," talk at Kagoshima University for The Physical Society of Japan 2007 Spring Meeting, 20pWG-4 (unpublished).
[43] K. Takeda, H. Hidaka, H. Kotegawa, T. C. Kobayashi, K. Shimizu, H. Harima, K. Fujiwara, K. Miyoshi, J. Takeuchi, Y. Ohishi, T. Adachi, M. Takata, E. Nishibori, M. Sakata, T. Watanuki, and O. Shimomura, Physica B **359**, 1312 (2005).
[44] K. Matsuno, T. Katsufuji, S. Mori, Y. Moritomo, A. Machida, E. Nishibori, M. Takata, M. Sakata, N. Yamamoto, and H. Takagi, J. Phys. Soc. Jpn. **70**, 1456 (2001).
[45] Y. Horibe, M. Shingu, K. Kurushima, H. Ishibashi, N. Ikeda, K. Kato, Y. Motome, N. Furukawa, S. Mori, and T. Katsufuji, Phys. Rev. Lett. **96**, 086406 (2006).
[46] N. Dragoe, L. Pinsard-Gaudart, J. P. Itie, A. Congeduti, P. Roy, S. Niitaka, H. Takagi, P. Lagarde, and A. M. Flank, High Press. Res. **26**, 427 (2006).
[47] L. Pinsard-Gaudart, N. Dragoe, P. Lagarde, A. Flank, J. Itie, A. Congeduti, P. Roy, S. Niitaka, and H. Takagi, Phys. Rev. B **76**, 045119 (2007).
[48] K. Fujiwara, H. Yoshioka, K. Miyoshi, J. Takeuchi, T. C. Kobayashi, and K. Amaya, Physica B **312–313**, 913 (2002).
[49] K. Fujiwara, K. Miyoshi, J. Takeuchi, Y. Shimaoka, and T. Kobayashi, J. Phys. Condens. Matter **16**, S615 (2004).
[50] H. Kimura, T. Moriwaki, S. Takahashi, H. Aoyagi, T. Matsushita, Y. Ishizawa, M. Masaki, S. Oishi, H. Ohkuma, T. Namba, M. Sakurai, S. Kimura, H. Okamura, H. Nakagawa, T. Takahashi, K. Fukui, K. Shinoda, Y. Kondoh, T. Sata, M. Okuno, M. Matsunami, R. Koyanagi, Y. Yoshimatsu, and T. Ishikawa, Nucl. Instrum. Methods Phys. Res., Sect. A **467–468**, 441 (2001).
[51] H. Ikemoto, Y. Moriwaki, T. Hirono, T. Kimura, S. Shinoda, K. Matsunami, M. Nagai, N. Nanba, T. Kobayashi, and K. Kimura, Infrared Phys. Technol. **45**, 369 (2004).
[52] The handmade microscope in the university is designed for the reflectivity measurements using DAC in the wide energy of 0.05–3 eV (from the FIR to VIS region). The optical system including the high-pressure unit and the refrigerator unit is installed in the high-vacuum chamber with diamond windows for optical transmission. The measurements in the wide energy range are feasible without changing optical windows in this system. The spectra were taken by the Fourier-transform- (FT-) type spectrometer of FT/IR-660 plus (JASCO) in the FIR-NIR region and by the grating-type spectrometer of MonoSpec 27 (Thermo Jarrell Ash) in the VIS region. The light sources of globar lamp and halogen lamp were used in the FIR-MIR region and the MIR-VIS region, respectively. The adopted detectors were the Si bolometer (Infrared Laboratory) in the FIR region and MCT (InfraRed associates) in the MIR-NIR region with the FT-type spectrometer, and photomultiplier R1767 (Hamamatsu Photonics) in the VIS region with the grating-type spectrometer. The sample temperature was controlled between 40 and 300 K. The *in situ* Au (or Al) deposition was performed to prepare the mirrored surface on the sample (covered with Au) without breaking the vacuum. The reflection from the mirrored surface was used as the reference under ambient pressure.
[53] K. Murata, K. Yokogawa, H. Yoshino, S. Klotz, P. Munsch, A. Irizawa, M. Nishiyama, K. Iizuka, T. Nanba, T. Okada, Y. Shiraga, and S. Aoyama, Rev. Sci. Instrum. **79**, 085101 (2008).
[54] The pressure test was done up to 12 GPa and the pressure distribution in the DAC was carefully checked by the authors (Ref. 53). From this, the gradient of pressure was found to be concentrated near the gasket, being much distant from the center. No critical deviation of the pressure was observed near the center within the area of 20 μm ϕ (10 μm distance from the center) which was comparable to the full width at half maximum of the focused FIR beam at BL43IR in SPring-8. Furthermore, as discussed in this paper, the MI transition of any polished sample became very sharp and the transition pressure became higher, as if the intermediate phase were absent. Thus, these results contradict such an apparent scenario that the intermediate phase explained in Fig. 3 originates from the pressure distribution, because the polished surface must have much more randomness and strain distribution compared to

the fractured surface and/or the as-grown surface. Consequently, we can safely conclude that the intermediate phase represents one of the intrinsic electronic states under high pressures in this compound.

[55]H. D. Lutz, B. Muller, and H. J. Steiner, J. Solid State Chem. **90**, 54 (1991).

[56]S. Suga, A. Sekiyama, H. Fujiwara, Y. Nakatsu, T. Miyamachi, S. Imada, P. Baltzer, S. Niitaka, H. Takagi, K. Yoshimura, M. Yabashi, K. Tamasaku, A. Higashiya, and T. Ishikawa, New J. Phys. **11**, 073025 (2009).

[57]S. Suga, A. Sekiyama, H. Fujiwara, Y. Nakatsu, J. Yamaguchi, M. Kimura, K. Murakami, S. Niitaka, H. Takagi, M. Yabashi, K. Tamasaku, A. Higashiya, T. Ishikawa, and I. Nekrasov, J. Phys. Soc. Jpn. **79**, 044711 (2010).

[58]A. Sekiyama, T. Iwasaki, K. Matsuda, Y. Saitoh, Y. Onuki, and S. Suga, Nature (London) **403**, 396 (2000).

[59]A. Sekiyama, H. Fujiwara, S. Imada, S. Suga, H. Eisaki, S. I. Uchida, K. Takegahara, H. Harima, Y. Saitoh, I. A. Nekrasov, G. Keller, D. E. Kondakov, A. V. Kozhevnikov, T. Pruschke, K. Held, D. Vollhardt, and V. I. Anisimov, Phys. Rev. Lett. **93**, 156402 (2004).

[60]S. Suga, A. Sekiyama, S. Imada, A. Shigemoto, A. Yamasaki, M. Tsunekawa, C. Dallera, L. Braicovich, T. Lee, O. Sakai, T. Ebihara, and Y. Onuki, J. Phys. Soc. Jpn. **74**, 2880 (2005).

[61]S. Das, A. Kreyssig, S. Nandi, A. I. Goldman, and D. C. Johnston, Phys. Rev. B **80**, 104401 (2009).

[62]S. Suga, A. Sekiyama, G. Funabashi, J. Yamaguchi, M. Kimura, M. Tsujibayashi, T. Uyama, H. Sugiyama, Y. Tomida, G. Kuwahara, S. Kitayama, K. Fukushima, K. Kimura, T. Yokoi, K. Murakami, H. Fujiwara, Y. Saitoh, L. Plucinski, and C. M. Schneider, Rev. Sci. Instrum. **81**, 105111 (2010).